EUROPEAN ORGANIZATION FOR NUCLEAR RESEARCH

CERN–EP/99–57

14 April 1999

Energy Dependence of Inclusive Spectra in e^+e^- Annihilation

DELPHI Collaboration

Abstract

Inclusive charged hadron distributions as obtaind from the DELPHI measurements at 130, 136, 161, 172 and 183 GeV are presented as a function of the variables rapidity, ξ_p, p and transversal momenta. Data are compared with event generators and with MLLA calculations, in order to examine the hypothesis of local parton hadron duality. The differential momentum spectra show an indication for coherence effects in the production of soft particles. The relation between the energy dependence of the charged multiplicity and the rapidity distribution is examined.

(Submitted to Phys. Lett. B)

P.Abreu[21], W.Adam[50], T.Adye[36], P.Adzic[11], Z.Albrecht[17], T.Alderweireld[2], G.D.Alekseev[16], R.Alemany[49], T.Allmendinger[17], P.P.Allport[22], S.Almehed[24], U.Amaldi[9], N.Amapane[45], S.Amato[47], E.G.Anassontzis[3], P.Andersson[44], A.Andreazza[9], S.Andringa[21], P.Antilogus[25], W-D.Apel[17], Y.Arnoud[9], B.Åsman[44], J-E.Augustin[25], A.Augustinus[9], P.Baillon[9], P.Bambade[19], F.Barao[21], G.Barbiellini[46], R.Barbier[25], D.Y.Bardin[16], G.Barker[17], A.Baroncelli[38], M.Battaglia[15], M.Baubillier[23], K-H.Becks[52], M.Begalli[6], A.Behrmann[52], P.Beilliere[8], Yu.Belokopytov[9,53], K.Belous[42], N.C.Benekos[31], A.C.Benvenuti[5], C.Berat[14], M.Berggren[25], D.Bertini[25], D.Bertrand[2], M.Besancon[39], M.Bigi[45], M.S.Bilenky[16], M-A.Bizouard[19], D.Bloch[10], H.M.Blom[30], M.Bonesini[27], W.Bonivento[27], M.Boonekamp[39], P.S.L.Booth[22], A.W.Borgland[4], G.Borisov[19], C.Bosio[41], O.Botner[48], E.Boudinov[30], B.Bouquet[19], C.Bourdarios[19], T.J.V.Bowcock[22], I.Boyko[16], I.Bozovic[11], M.Bozzo[13], P.Branchini[38], T.Brenke[52], R.A.Brenner[48], P.Bruckman[18], J-M.Brunet[8], L.Bugge[32], T.Buran[32], T.Burgsmueller[52], B.Buschbeck[50], P.Buschmann[52], S.Cabrera[49], M.Caccia[27], M.Calvi[27], T.Camporesi[9], V.Canale[37], F.Carena[9], L.Carroll[22], C.Caso[13], M.V.Castillo Gimenez[49], A.Cattai[9], F.R.Cavallo[5], V.Chabaud[9], M.Chapkin[42], Ph.Charpentier[9], L.Chaussard[25], P.Checchia[35], G.A.Chelkov[16], R.Chierici[45], P.Chliapnikov[42], P.Chochula[7], V.Chorowicz[25], J.Chudoba[29], K.Cieslik[18], P.Collins[9], R.Contri[13], E.Cortina[49], G.Cosme[19], F.Cossutti[9], J-H.Cowell[22], H.B.Crawley[1], D.Crennell[36], S.Crepe[14], G.Crosetti[13], J.Cuevas Maestro[33], S.Czellar[15], M.Davenport[9], W.Da Silva[23], A.Deghorain[2], G.Della Ricca[46], P.Delpierre[26], N.Demaria[9], A.De Angelis[9], W.De Boer[17], C.De Clercq[2], B.De Lotto[46], A.De Min[35], L.De Paula[47], H.Dijkstra[9], L.Di Ciaccio[37,9], J.Dolbeau[8], K.Doroba[51], M.Dracos[10], J.Drees[52], M.Dris[31], A.Duperrin[25], J-D.Durand[9], G.Eigen[4], T.Ekelof[48], G.Ekspong[44], M.Ellert[48], M.Elsing[9], J-P.Engel[10], B.Erzen[43], M.Espirito Santo[21], E.Falk[24], G.Fanourakis[11], D.Fassouliotis[11], J.Fayot[23], M.Feindt[17], A.Fenyuk[42], P.Ferrari[27], A.Ferrer[49], E.Ferrer-Ribas[19], F.Ferro[13], S.Fichet[23], A.Firestone[1], U.Flagmeyer[52], H.Foeth[9], E.Fokitis[31], F.Fontanelli[13], B.Franek[36], A.G.Frodesen[4], R.Fruhwirth[50], F.Fulda-Quenzer[19], J.Fuster[49], A.Galloni[22], D.Gamba[45], S.Gamblin[19], M.Gandelman[47], C.Garcia[49], C.Gaspar[9], M.Gaspar[47], U.Gasparini[35], Ph.Gavillet[9], E.N.Gazis[31], D.Gele[10], N.Ghodbane[25], I.Gil[49], F.Glege[52], R.Gokieli[9,51], B.Golob[43], G.Gomez-Ceballos[40], P.Goncalves[21], I.Gonzalez Caballero[40], G.Gopal[36], L.Gorn[1,54], M.Gorski[51], Yu.Gouz[42], V.Gracco[13], J.Grahl[1], E.Graziani[38], C.Green[22], H-J.Grimm[17], P.Gris[39], G.Grosdidier[19], K.Grzelak[51], M.Gunther[48], J.Guy[36], F.Hahn[9], S.Hahn[52], S.Haider[9], A.Hallgren[48], K.Hamacher[52], J.Hansen[32], F.J.Harris[34], V.Hedberg[24], S.Heising[17], J.J.Hernandez[49], P.Herquet[2], H.Herr[9], T.L.Hessing[34], J.-M.Heuser[52], E.Higon[49], S-O.Holmgren[44], P.J.Holt[34], S.Hoorelbeke[2], M.Houlden[22], J.Hrubec[50], K.Huet[2], G.J.Hughes[22], K.Hultqvist[44], J.N.Jackson[22], R.Jacobsson[9], P.Jalocha[9], R.Janik[7], Ch.Jarlskog[24], G.Jarlskog[24], P.Jarry[39], B.Jean-Marie[19], E.K.Johansson[44], P.Jonsson[25], C.Joram[9], P.Juillot[10], F.Kapusta[23], K.Karafasoulis[11], S.Katsanevas[25], E.C.Katsoufis[31], R.Keranen[17], B.P.Kersevan[43], B.A.Khomenko[16], N.N.Khovanski[16], A.Kiiskinen[15], B.King[22], A.Kinvig[22], N.J.Kjaer[30], O.Klapp[52], H.Klein[9], P.Kluit[30], P.Kokkinias[11], M.Koratzinos[9], V.Kostioukhine[42], C.Kourkoumelis[3], O.Kouznetsov[39], M.Krammer[50], E.Kriznic[43], P.Krstic[11], Z.Krumstein[16], P.Kubinec[7], J.Kurowska[51], K.Kurvinen[15], J.W.Lamsa[1], D.W.Lane[1], P.Langefeld[52], J-P.Laugier[39], R.Lauhakangas[15], F.Ledroit[14], V.Lefebure[2], L.Leinonen[44], A.Leisos[11], R.Leitner[29], G.Lenzen[52], V.Lepeltier[19], T.Lesiak[18], M.Lethuillier[39], J.Libby[34], D.Liko[9], A.Lipniacka[44], I.Lippi[35], B.Loerstad[24], J.G.Loken[34], J.H.Lopes[47], J.M.Lopez[40], R.Lopez-Fernandez[14], D.Loukas[11], P.Lutz[39], L.Lyons[34], J.MacNaughton[50], J.R.Mahon[6], A.Maio[21], A.Malek[52], T.G.M.Malmgren[44], S.Maltezos[31], V.Malychev[16], F.Mandl[50], J.Marco[40], R.Marco[40], B.Marechal[47], M.Margoni[35], J-C.Marin[9], C.Mariotti[9], A.Markou[11], C.Martinez-Rivero[19], F.Martinez-Vidal[49], S.Marti i Garcia[9], J.Masik[12], N.Mastroyiannopoulos[11], F.Matorras[40], C.Matteuzzi[27], G.Matthiae[37], F.Mazzucato[35], M.Mazzucato[35], M.Mc Cubbin[22], R.Mc Kay[1], R.Mc Nulty[22], G.Mc Pherson[22], C.Meroni[27], W.T.Meyer[1], E.Migliore[45], L.Mirabito[25], W.A.Mitaroff[50], U.Mjoernmark[24], T.Moa[44], M.Moch[17], R.Moeller[28], K.Moenig[9], M.R.Monge[13], X.Moreau[23], P.Morettini[13], G.Morton[34], U.Mueller[52], K.Muenich[52], M.Mulders[30], C.Mulet-Marquis[14], R.Muresan[24], W.J.Murray[36], B.Muryn[14,18], G.Myatt[34], T.Myklebust[32], F.Naraghi[14], M.Nassiakou[11], F.L.Navarria[5], S.Navas[49], K.Nawrocki[51], P.Negri[27], S.Nemecek[12], N.Neufeld[9], N.Neumeister[50], R.Nicolaidou[39], B.S.Nielsen[28], M.Nikolenko[10,16], V.Nomokonov[15], A.Normand[22], A.Nygren[24], V.Obraztsov[42], A.G.Olshevski[16], A.Onofre[21], R.Orava[15], G.Orazi[10], K.Osterberg[15], A.Ouraou[39], M.Paganoni[27], S.Paiano[5], R.Pain[23], R.Paiva[21], J.Palacios[34], H.Palka[18], Th.D.Papadopoulou[31,9], K.Papageorgiou[11], L.Pape[9], C.Parkes[9], F.Parodi[13], U.Parzefall[22], A.Passeri[38], O.Passon[52], M.Pegoraro[35], L.Peralta[21], M.Pernicka[50], A.Perrotta[5], C.Petridou[46], A.Petrolini[13], H.T.Phillips[36], F.Pierre[39], M.Pimenta[21], E.Piotto[27], T.Podobnik[43], M.E.Pol[6], G.Polok[18], P.Poropat[46], V.Pozdniakov[16], P.Privitera[37], N.Pukhaeva[16], A.Pullia[27], D.Radojicic[34], S.Ragazzi[27], H.Rahmani[31], P.N.Ratoff[20], A.L.Read[32], P.Rebecchi[9], N.G.Redaelli[27], M.Regler[50], D.Reid[30], R.Reinhardt[52], P.B.Renton[34], L.K.Resvanis[3], F.Richard[19], J.Ridky[12], G.Rinaudo[45], O.Rohne[32], A.Romero[45], P.Ronchese[35], E.I.Rosenberg[1], P.Rosinsky[7], P.Roudeau[19], T.Rovelli[5], Ch.Royon[39], V.Ruhlmann-Kleider[39], A.Ruiz[40], H.Saarikko[15], Y.Sacquin[39], A.Sadovsky[16], G.Sajot[14], J.Salt[49], D.Sampsonidis[11], M.Sannino[13], H.Schneider[17], Ph.Schwemling[23], B.Schwering[52], U.Schwickerath[17], M.A.E.Schyns[52], F.Scuri[46], P.Seager[20], Y.Sedykh[16], A.M.Segar[34], R.Sekulin[36], R.C.Shellard[6], A.Sheridan[22], M.Siebel[52], L.Simard[39], F.Simonetto[35], A.N.Sisakian[16], G.Smadja[25], N.Smirnov[42], O.Smirnova[24], G.R.Smith[36], A.Sopczak[17], R.Sosnowski[51], T.Spassov[21], E.Spiriti[38], P.Sponholz[52], S.Squarcia[13], C.Stanescu[38], S.Stanic[43], K.Stevenson[34], A.Stocchi[19], J.Strauss[50], R.Strub[10], B.Stugu[4], M.Szczekowski[51], M.Szeptycka[51], T.Tabarelli[27], O.Tchikilev[42], F.Tegenfeldt[48], F.Terranova[27], J.Thomas[34], J.Timmermans[30], N.Tinti[5], L.G.Tkatchev[16], S.Todorova[10], A.Tomaradze[2], B.Tome[21], A.Tonazzo[9], L.Tortora[38], G.Transtromer[24], D.Treille[9], G.Tristram[8], M.Trochimczuk[51], C.Troncon[27],

A.Tsirou[9], M-L.Turluer[39], I.A.Tyapkin[16], S.Tzamarias[11], O.Ullaland[9], V.Uvarov[42], G.Valenti[5], E.Vallazza[46], G.W.Van Apeldoorn[30], P.Van Dam[30], J.Van Eldik[30], A.Van Lysebetten[2], N.Van Remortel[2], I.Van Vulpen[30], N.Vassilopoulos[34], G.Vegni[27], L.Ventura[35], W.Venus[36,9], F.Verbeure[2], M.Verlato[35], L.S.Vertogradov[16], V.Verzi[37], D.Vilanova[39], L.Vitale[46], E.Vlasov[42], A.S.Vodopyanov[16], C.Vollmer[17], G.Voulgaris[3], V.Vrba[12], H.Wahlen[52], C.Walck[44], C.Weiser[17], D.Wicke[52], J.H.Wickens[2], G.R.Wilkinson[9], M.Winter[10], M.Witek[18], G.Wolf[9], J.Yi[1], O.Yushchenko[42], A.Zaitsev[42], A.Zalewska[18], P.Zalewski[51], D.Zavrtanik[43], E.Zevgolatakos[11], N.I.Zimin[16,24], G.C.Zucchelli[44], G.Zumerle[35]

[1] Department of Physics and Astronomy, Iowa State University, Ames IA 50011-3160, USA
[2] Physics Department, Univ. Instelling Antwerpen, Universiteitsplein 1, BE-2610 Wilrijk, Belgium
and IIHE, ULB-VUB, Pleinlaan 2, BE-1050 Brussels, Belgium
and Faculté des Sciences, Univ. de l'Etat Mons, Av. Maistriau 19, BE-7000 Mons, Belgium
[3] Physics Laboratory, University of Athens, Solonos Str. 104, GR-10680 Athens, Greece
[4] Department of Physics, University of Bergen, Allégaten 55, NO-5007 Bergen, Norway
[5] Dipartimento di Fisica, Università di Bologna and INFN, Via Irnerio 46, IT-40126 Bologna, Italy
[6] Centro Brasileiro de Pesquisas Físicas, rua Xavier Sigaud 150, BR-22290 Rio de Janeiro, Brazil
and Depto. de Física, Pont. Univ. Católica, C.P. 38071 BR-22453 Rio de Janeiro, Brazil
and Inst. de Física, Univ. Estadual do Rio de Janeiro, rua São Francisco Xavier 524, Rio de Janeiro, Brazil
[7] Comenius University, Faculty of Mathematics and Physics, Mlynska Dolina, SK-84215 Bratislava, Slovakia
[8] Collège de France, Lab. de Physique Corpusculaire, IN2P3-CNRS, FR-75231 Paris Cedex 05, France
[9] CERN, CH-1211 Geneva 23, Switzerland
[10] Institut de Recherches Subatomiques, IN2P3 - CNRS/ULP - BP20, FR-67037 Strasbourg Cedex, France
[11] Institute of Nuclear Physics, N.C.S.R. Demokritos, P.O. Box 60228, GR-15310 Athens, Greece
[12] FZU, Inst. of Phys. of the C.A.S. High Energy Physics Division, Na Slovance 2, CZ-180 40, Praha 8, Czech Republic
[13] Dipartimento di Fisica, Università di Genova and INFN, Via Dodecaneso 33, IT-16146 Genova, Italy
[14] Institut des Sciences Nucléaires, IN2P3-CNRS, Université de Grenoble 1, FR-38026 Grenoble Cedex, France
[15] Helsinki Institute of Physics, HIP, P.O. Box 9, FI-00014 Helsinki, Finland
[16] Joint Institute for Nuclear Research, Dubna, Head Post Office, P.O. Box 79, RU-101 000 Moscow, Russian Federation
[17] Institut für Experimentelle Kernphysik, Universität Karlsruhe, Postfach 6980, DE-76128 Karlsruhe, Germany
[18] Institute of Nuclear Physics and University of Mining and Metalurgy, Ul. Kawiory 26a, PL-30055 Krakow, Poland
[19] Université de Paris-Sud, Lab. de l'Accélérateur Linéaire, IN2P3-CNRS, Bât. 200, FR-91405 Orsay Cedex, France
[20] School of Physics and Chemistry, University of Lancaster, Lancaster LA1 4YB, UK
[21] LIP, IST, FCUL - Av. Elias Garcia, 14-1^{o}, PT-1000 Lisboa Codex, Portugal
[22] Department of Physics, University of Liverpool, P.O. Box 147, Liverpool L69 3BX, UK
[23] LPNHE, IN2P3-CNRS, Univ. Paris VI et VII, Tour 33 (RdC), 4 place Jussieu, FR-75252 Paris Cedex 05, France
[24] Department of Physics, University of Lund, Sölvegatan 14, SE-223 63 Lund, Sweden
[25] Université Claude Bernard de Lyon, IPNL, IN2P3-CNRS, FR-69622 Villeurbanne Cedex, France
[26] Univ. d'Aix - Marseille II - CPP, IN2P3-CNRS, FR-13288 Marseille Cedex 09, France
[27] Dipartimento di Fisica, Università di Milano and INFN, Via Celoria 16, IT-20133 Milan, Italy
[28] Niels Bohr Institute, Blegdamsvej 17, DK-2100 Copenhagen Ø, Denmark
[29] NC, Nuclear Centre of MFF, Charles University, Areal MFF, V Holesovickach 2, CZ-180 00, Praha 8, Czech Republic
[30] NIKHEF, Postbus 41882, NL-1009 DB Amsterdam, The Netherlands
[31] National Technical University, Physics Department, Zografou Campus, GR-15773 Athens, Greece
[32] Physics Department, University of Oslo, Blindern, NO-1000 Oslo 3, Norway
[33] Dpto. Fisica, Univ. Oviedo, Avda. Calvo Sotelo s/n, ES-33007 Oviedo, Spain
[34] Department of Physics, University of Oxford, Keble Road, Oxford OX1 3RH, UK
[35] Dipartimento di Fisica, Università di Padova and INFN, Via Marzolo 8, IT-35131 Padua, Italy
[36] Rutherford Appleton Laboratory, Chilton, Didcot OX11 OQX, UK
[37] Dipartimento di Fisica, Università di Roma II and INFN, Tor Vergata, IT-00173 Rome, Italy
[38] Dipartimento di Fisica, Università di Roma III and INFN, Via della Vasca Navale 84, IT-00146 Rome, Italy
[39] DAPNIA/Service de Physique des Particules, CEA-Saclay, FR-91191 Gif-sur-Yvette Cedex, France
[40] Instituto de Fisica de Cantabria (CSIC-UC), Avda. los Castros s/n, ES-39006 Santander, Spain
[41] Dipartimento di Fisica, Università degli Studi di Roma La Sapienza, Piazzale Aldo Moro 2, IT-00185 Rome, Italy
[42] Inst. for High Energy Physics, Serpukov P.O. Box 35, Protvino, (Moscow Region), Russian Federation
[43] J. Stefan Institute, Jamova 39, SI-1000 Ljubljana, Slovenia and Laboratory for Astroparticle Physics,
Nova Gorica Polytechnic, Kostanjeviska 16a, SI-5000 Nova Gorica, Slovenia,
and Department of Physics, University of Ljubljana, SI-1000 Ljubljana, Slovenia
[44] Fysikum, Stockholm University, Box 6730, SE-113 85 Stockholm, Sweden
[45] Dipartimento di Fisica Sperimentale, Università di Torino and INFN, Via P. Giuria 1, IT-10125 Turin, Italy
[46] Dipartimento di Fisica, Università di Trieste and INFN, Via A. Valerio 2, IT-34127 Trieste, Italy
and Istituto di Fisica, Università di Udine, IT-33100 Udine, Italy
[47] Univ. Federal do Rio de Janeiro, C.P. 68528 Cidade Univ., Ilha do Fundão BR-21945-970 Rio de Janeiro, Brazil
[48] Department of Radiation Sciences, University of Uppsala, P.O. Box 535, SE-751 21 Uppsala, Sweden
[49] IFIC, Valencia-CSIC, and D.F.A.M.N., U. de Valencia, Avda. Dr. Moliner 50, ES-46100 Burjassot (Valencia), Spain
[50] Institut für Hochenergiephysik, Österr. Akad. d. Wissensch., Nikolsdorfergasse 18, AT-1050 Vienna, Austria
[51] Inst. Nuclear Studies and University of Warsaw, Ul. Hoza 69, PL-00681 Warsaw, Poland
[52] Fachbereich Physik, University of Wuppertal, Postfach 100 127, DE-42097 Wuppertal, Germany
[53] On leave of absence from IHEP Serpukhov
[54] Now at University of Florida

1 Introduction

This paper presents inclusive charged hadron spectra measured by DELPHI at centre-of-mass energies from 130 to 183 GeV. The results are compared to Z data and to the measurements from low energy experiments.

Inclusive stable hadron spectra are highly sensitive to properties of the hadronization process and to resonance decays as well as to details of the parton shower. They depend on the amount of large angle and collinear gluon radiation and on the coherence of gluon radiation. The measurements therefore provide rigid constraints on models of the hadronization process.

Direct comparisons of inclusive distributions with QCD calculations suffer from their dependence on infrared and collinear divergences: finite predictions in the framework of perturbative QCD can only be obtained by introducing a cut-off in momentum. Moreover, to compare calculations of spectra to experimental data one has to assume that parton distributions are proportional to inclusive hadron distributions; this is frequently referred to as "local parton hadron duality" (LPHD) [1]. Studies of the energy evolution of inclusive spectra provide new information because the divergent terms can be factorized out and the energy dependence can be more directly compared to perturbative QCD predictions.

In Section 2 the selection of hadronic events, the reconstruction of the centre-of-mass energy, the correction procedures applied to the data and especially the corrections for the background from W^+W^- events are briefly discussed. In Section 3 the inclusive spectra as measured by DELPHI are compared with the predictions from different Monte Carlo models. Results concerning the energy dependence of the rapidity distribution and the distributions of scaled and absolute momenta are presented. A brief summary is given in Section 4 .

2 Selection and correction of hadronic data

The analysis is based on data taken with the DELPHI detector at 130, 136, 161, 172 and 183 GeV. The measurements at 130 and 136 GeV are averaged and labeled as 133 GeV. The integrated luminosity corresponds to about $10\,\mathrm{pb}^{-1}$ each for the 133, 161 and 172 GeV data and $54\,\mathrm{pb}^{-1}$ for the 183 GeV data.

DELPHI is a hermetic detector with a solenoidal magnetic field of 1.2 T. The tracking detectors, which lie in front of the electromagnetic calorimeters, are a silicon micro vertex detector VD, a combined jet/proportional chamber inner detector ID, a time projection chamber TPC as the major tracking device, and the streamer tube outer detector OD in the barrel region. The forward region is covered by the drift chamber detectors FCA and FCB.

The electromagnetic calorimeters are the high density projection chamber HPC in the barrel, the lead glass calorimeter FEMC in the forward region and the STIC next to the beam pipe. Detailed information about the construction and performance of DELPHI can be found in [2,3]. The standard system of coordinates of DELPHI is also defined in [3].

In order to select well measured charged particle tracks, the cuts given in the upper part of Table 1 have been applied. The cuts in the lower part of the table have been used to select hadronic events $e^+e^- \to Z/\gamma \to q\bar{q}$ and to suppress background processes such as two photon interactions, beam gas and beam wall interactions, leptonic final states, and,

charged particle selection	all energies			
p[GeV]	$0.2 \leq p \leq 100$			
$\Delta p/p$	≤ 1			
θ	$20^\circ \leq \theta \leq 160^\circ$			
track length	≥ 30cm			
$\Delta_{r\phi}$	≤ 4cm			
Δ_z	≤ 10cm			
event selection				
$\theta_{\rm Thrust}$	$30^\circ \leq \theta \leq 150^\circ$			
$E_{\rm tot}$	$\geq 50\%\ E_{CM}$			
$\sqrt{s'}$	$\geq 90\%\ E_{CM}$			
	133 GeV	161 GeV	172 GeV	183 GeV
$N_{\rm ch}$	$7 \leq N_{\rm ch}$	$8 \leq N_{\rm ch} \leq 38$	$8 \leq N_{\rm ch} \leq 40$	$8 \leq N_{ch} \leq 42$
$B_{\rm min}$	-	$\leq .09$	$\leq .08$	$\leq .07$

Table 1: Selection of charged particles and events. p is the momentum, θ is the polar angle with respect to the beam (likewise $\theta_{\rm Thrust}$ for the thrust axis $n_{\rm T}$), $\Delta_{r\phi}$ and Δ_z are the distances to the interaction point in $r\phi$ (radial distance to beam axis and azimuthal angle) and z (distance along the beam axis) respectively. $N_{\rm ch}$ is the number of charged particles, $E_{\rm tot}$ the total energy carried by all selected particles, s' the square of the reconstructed centre-of-mass energy, as reduced by initial state radiation. E_{CM} is the nominal LEP energy, $B_{{\rm m}in}$ is the minimal jet broadening (see text).

most important for the LEP2 analysis, events with large initial state radiation (ISR) and W pair production. At energies above the Z peak, initial fermions may radiate one or more photons before they interact, such that the effective centre-of-mass energy for the collision is the mass of the Z. These "radiative return events" are the dominant part of the cross–section. The initial state radiation (ISR) is typically aligned along the beam direction and the photons are only rarely identified inside the detector. In order to evaluate the effective centre-of-mass energy ($\sqrt{s'}$) of an event, considering ISR, an algorithm is used that is based on a constrained fit method using four–momenta of jets and taking energy and momentum conservation into account [5].

The production of W pairs occurs above the threshold of 161 GeV . Since the topological signatures of QCD four–jet events and hadronic WW events (and other four fermion background) are very similar, no highly efficient separation, of the two classes of events is possible. As a suitable discriminant variable for performing the separation the shape $B_{{\rm m}in}$ is chosen, which is defined as $B_{{\rm m}in} = \min\{B_+, B_-\}$ with:

$$B_\pm = \frac{\sum_{\pm\vec{p}_i\cdot\hat{n}_{\rm T}>0} |\vec{p}_i \times \hat{n}_{\rm T}|}{2\sum |\vec{p}_i|},$$

where the sum runs over all selected particles. The cut applied to the maximum charged multiplicity also discards W events. The event selection cuts (table 1) are optimized in order to maximize the purity with respect to the $\sqrt{s'}$ selection, the efficiency of collecting high energy $q\bar{q}$ events and the WW rejection. Furthermore the QCD bias introduced by the $B_{{\rm m}in}$ cut is minimized. Table 2 shows the efficiency of the WW rejection and the remaining contamination. This WW contribution was evaluated by Monte Carlo simulation and subtracted from the data. The small effect of Z pair production was also

	133 GeV	161 GeV	172 GeV	183 GeV
σ_{WW}[pb]	-	3.3	12.1	15.4
WW rejection efficiency	-	0.77	0.82	0.84
WW background	-	7.6 ± 0.3	21.7 ± 0.5	130.7 ± 2.3
$\sqrt{s'}$ purity	0.87	0.94	0.93	0.95
selected events	762	332	253	1126

Table 2: Cross– section of W pair production, efficiency of WW rejection and number of remaining WW events. These are subtracted assuming the background to be distributed as in the simulation. The last row shows the number of selected hadronic events entering in this analysis. Monte Carlo studies demonstrate that other background sources give negligible contributions.

taken into account for the 183 GeV data. Two photon events are strongly suppressed by the cuts. Leptonic background can also be neglected in this analysis.

The influence of detector effects was studied by passing generated events (PYTHIA[4] tuned by DELPHI [6]) through a full detector simulation (DELSIM [3]). Such Monte Carlo events were processed with the same cuts as real data. They are identified by the subscipt "acc" in the following. The tuned generator prediction is denoted as "gen". In order to correct for cuts, detector and ISR effects, a bin by bin correction factor (acceptance correction) was applied to the data. For bin f of histogram h it is defined as:

$$C = \frac{h(f)_{\mathrm{gen,noISR}}}{h(f)_{\mathrm{acc}}}\,. \tag{1}$$

For $h(f)_{\mathrm{acc}}$ all cuts were applied, for $h(f)_{\mathrm{gen,noISR}}$ a total ISR of less than 1 GeV was demanded.

3 Results

Comparisons of inclusive distributions with model expectations are presented as a function of: the logarithm of the scaled hadron momentum $\xi_p = \ln(1/x_p)$ (with $x_p = p/p_{\mathrm{beam}}$), the rapidity with respect to the thrust axis $y_t = 0.5 \cdot \ln((E+p_{\parallel})/(E-p_{\parallel}))$ as well as the two momentum components (p_t^{in}, p_t^{out}) transverse to the thrust axis which lie in and perpendicular to the plane of the event. E and p are the particle momenta and energies respectively. All energies have been computed assuming the charged particles to be pions, and the momenta of neutral particles assuming them to be massless.

Figures 1 and 2 show a selection of the ξ_p, y_t, p_t^{in} and p_t^{out} spectra as determined from the high energy data. The data are compared to the JETSET 7.4, HERWIG 5.8 and ARIADNE 4.08 fragmentation models as tuned by DELPHI [6]. The shaded areas display the size of the WW (above 161 GeV) and ZZ (above 183 GeV) background which was subtracted from the data. The upper inset in these plots shows the correction factor applied to the data. The lower inset presents the ratio of the high energy data to the corresponding results at the Z. This ratio is again compared to the model predictions.

The models describe well all inclusive spectra measured at the high energies and also the energy evolution from the Z peak (see the lower inset of Fig. 1 and 2). The most prominent change in the ξ_p distribution (Fig. 2 a and c) is an increase at large ξ_p (i.e. low x_p). In the rapidity distribution (Fig. 2 b and d) the expected increase of the width of

the distribution is clearly observed together with a slight increase of the plateau height. These changes and the strong increase in the transverse momentum distributions at large $p_\perp$ (Fig. 1b and d) are due to stronger gluon radiation at the higher energies.

3.1 Energy Evolution of the Rapidity Distribution

In Fig. 3 a) rapidity distributions obtained from DELPHI at energies from 91 [6] to 183 GeV are compared to earlier results from 14 to 57 GeV[7–10]. The full lines displays the predictions of the JETSET model (tuned at the Z energy [6]), which agrees well with the DELPHI data. While the 35 GeV TASSO [7] and 29 GeV MARK II [8] data are well described, the AMY [9] and low energy TASSO data [10] deviate significantly from the model prediction.

Contrary to the simple parton model expectation not only the width of the distribution, but also the height of the rapidity plateau increases with the centre-of-mass energy. In order to describe the energy dependence the quantity "height of the rapidity plateau" is defined as the average value of the measured distributions in the range $0 \leq y \leq r \cdot (1/N\ dn/dy)_{\max}$. The central value is obtained by averaging the results for $r = 0.85, 0.90, 0.95$. The error was estimated by the quadratic sum of the single statistical error and the spread of the different fit results. The width of the distribution was taken to be the rapidity value at which the distribution has fallen to half of the plateau height. Its error corresponds to the uncertainty of the plateau height.

Fig. 3 b) shows the energy evolution of these parameters from 14 to 183 GeV (two lower curves). The dashed and dotted lines are parametrisations with a function of the form $a_i \cdot E_{\rm CM}^{b_i}$. The upper curve is the product of those two parametrisations.

Since the product of width and height of the rapidity distribution is expected to give roughly the area below it and hence the charged multiplicity, this line is compared with measurements of $< N_{\rm ch} >$ [11–16]. The double logarithmic presentation allows the slopes of the width and height variation with energy to be compared. The straight line fit of the form $a_i \cdot E_{\rm CM}^{b_i}$, as presented in Fig. 3 b), yields $b_w = 0.159 \pm 0.005$ for the width and $b_h = 0.252 \pm 0.004$ for the height. The ratio of $b_h/b_w \approx 1.5$ indicates that the multiplicity increase is mainly due to the increase of particles with small rapidity, and to a smaller extent due to the growth in width of the rapidity distribution.

3.2 Energy Dependence of ξ_p and ξ^*

The shape of the partonic ξ_p distribution, as calculated in the Modified Leading Log Approximation (MLLA), exhibits the characteristic "hump backed" plateau due to suppression of soft gluon radiation [17]. The calculation in the "limited spectrum" approximation ($\Lambda_{\rm eff} = Q_0$) can be well expressed by a distorted Gaussian (2):

$$\frac{1}{N_{\rm event}}\frac{dn}{d\xi_p} = \frac{N(Y)}{\sigma\sqrt{2\pi}} \exp\left(\frac{k}{8} - \frac{s\delta}{2} - \frac{(2+k)\delta^2}{4} + \frac{s\delta^3}{6} + \frac{k\delta^4}{24}\right) \qquad (2)$$

with $\delta = (\xi - < \xi >)/(\sigma)$, $< \xi >$ the mean, σ the width, s the skewness and k the kurtosis of the distribution. $N(Y)$ is an energy dependent normalization factor. With the number of participating quark flavours, N_F, $\beta = 11 - 2N_F/3$, $\rho = 11 + 2N_F/27$ and $\omega = 1 + N_F/27$ one obtains for *quark jets* [18]:

$$< \xi > \ = \ \frac{1}{2}Y \cdot \left(1 + \frac{\rho}{24}\sqrt{\frac{48}{\beta Y}}\right) \cdot \left(1 - \frac{\omega}{6Y}\right) + \mathcal{O}(1)$$

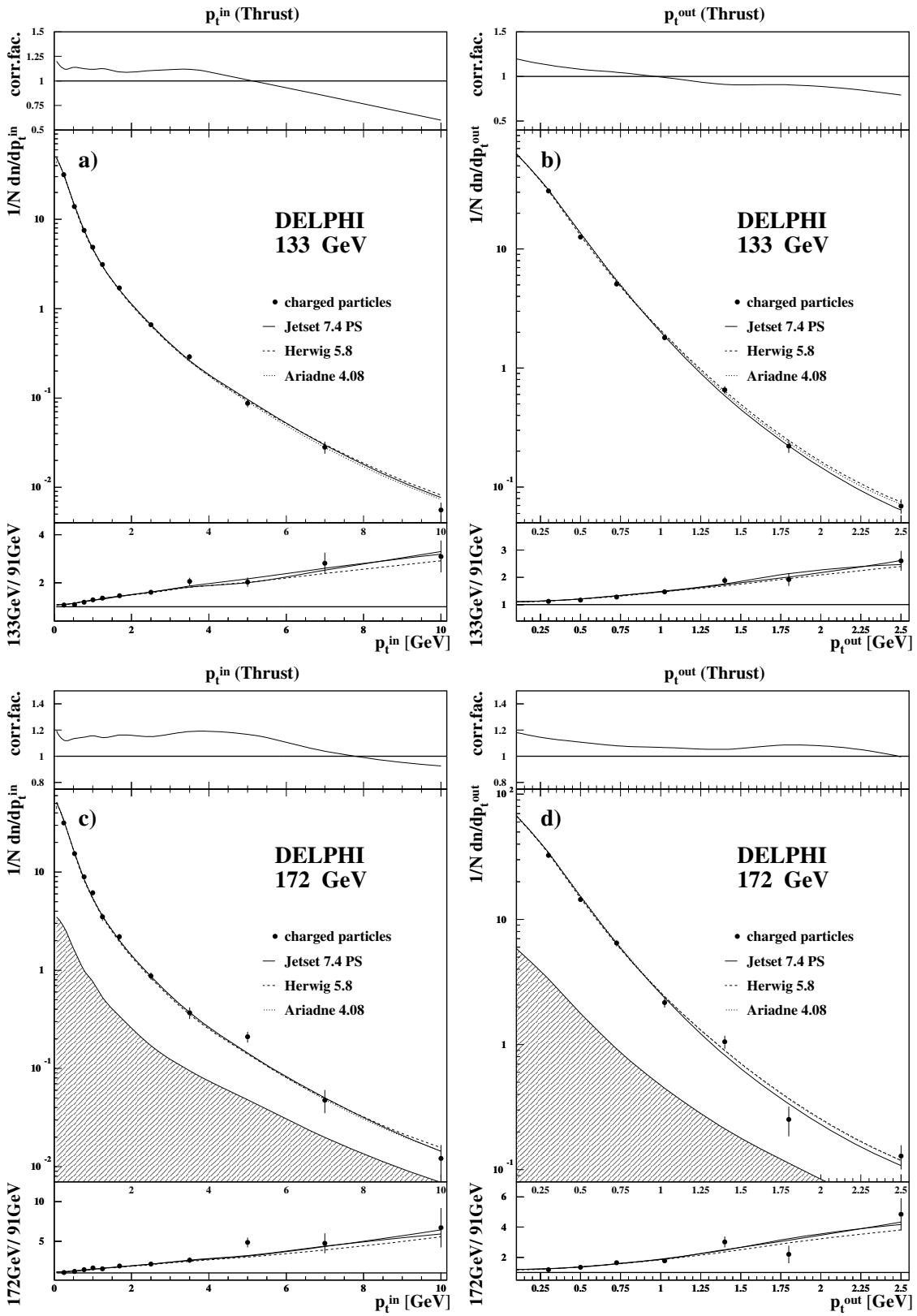

Figure 1: $p_t^{\rm in}$ and $p_t^{\rm out}$ distributions for 133 and 172 GeV. The shaded areas for the 172 GeV data display the WW background which has been subtracted from the data. The upper insets in these plots show the correction factor applied to the data. The lower insets present the ratio of the high energy data to the corresponding results at the Z.

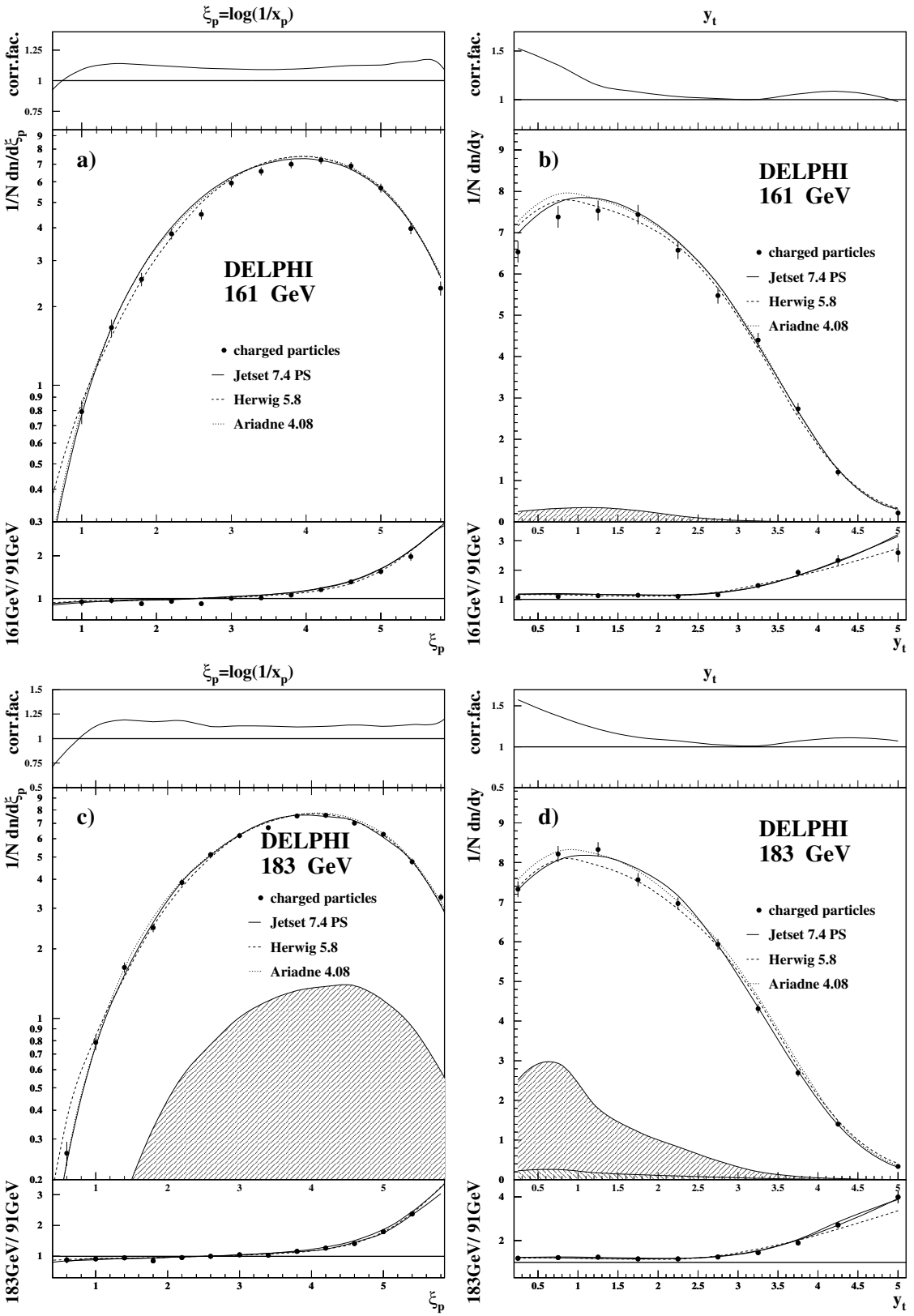

Figure 2: ξ_p and rapidity distribution at 161 and 183 GeV. The shaded areas display the WW background (for the 183 GeV data, also the small contribution from ZZ bachground is shown) which has been subtracted from the data; the WW background in (a) is below the smallest ordinate value. The upper insets in these plots show the correction factor applied to the data. The lower insets present the ratio of the high energy data to the corresponding results at the Z.

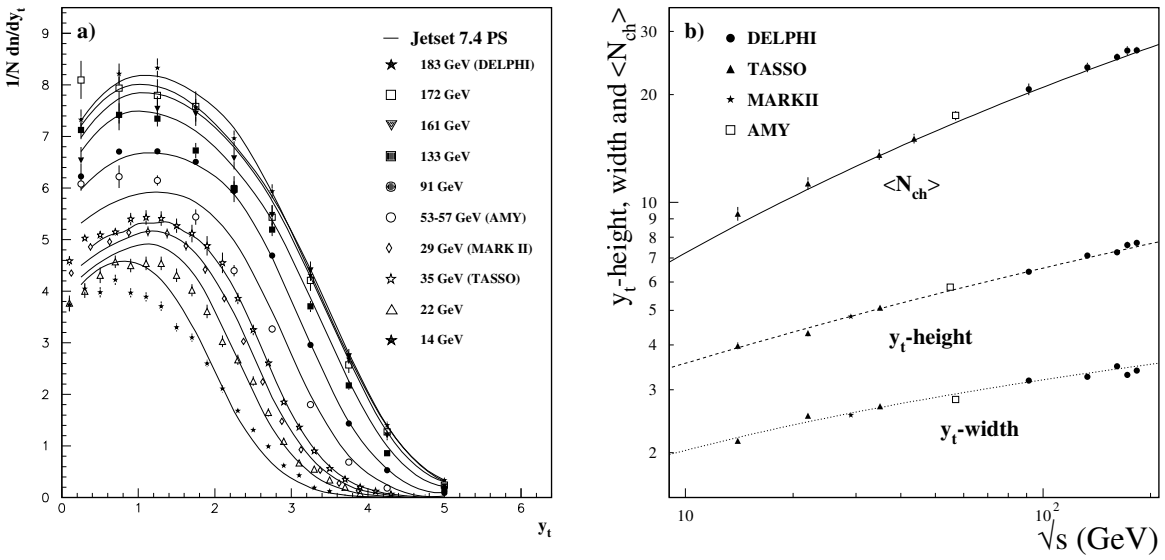

Figure 3: a) Rapidity distributions for various energies. b) Energy dependence of $< N_{\rm ch} >$, plateau height and width of the rapidity distribution. The two lower curves are parametrisations of these measurements, while the upper curve is the product of these two parametrisations.

$$
\begin{aligned}
\sigma &= \sqrt{\frac{Y}{3}} \cdot \left(\frac{\beta Y}{48}\right)^{1/4} \cdot \left(1 - \frac{\beta}{64}\sqrt{\frac{48}{\beta Y}}\right) \cdot \left(1 + \frac{\omega}{8Y}\right) + \mathcal{O}(Y^{-1/4}) \\
s &= -\frac{\rho}{16}\sqrt{\frac{3}{Y}} \cdot \left(\frac{48}{\beta Y}\right)^{1/4} \cdot \left(1 + \frac{\omega}{4Y}\right) + \mathcal{O}(Y^{-5/4}) \\
k &= -\frac{27}{5Y} \cdot \left(\sqrt{\frac{\beta Y}{48}} - \frac{\beta}{24}\right) \cdot \left(1 + \frac{5\omega}{12Y}\right) + \mathcal{O}(Y^{-3/2})
\end{aligned}
$$

Here $Y = \ln(E_{\rm beam}/\Lambda_{\rm eff})$ and $\Lambda_{\rm eff}$ is an effective scale parameter. $\Lambda_{\rm eff}$, the overall normalization N and the additional constant term of $\mathcal{O}(1)$ in $< \xi >$ are the free parameters in this expression which is valid in the region around the maximum, and contains high energy approximations. Using the Local Parton Hadron Duality (LPHD) hypothesis this shape can directly be adapted to the measured hadron spectrum [1]. In Fig. 4 the ξ_p distributions as determined from LEP2 data are compared to the DELPHI results at the Z [6] and to other experiments [12,19]. The full lines are the results of a simultaneous fit of the Fong-Webber parametrisation (2) to all but the Z data yielding χ^2/dof=92/89. The Z data are left out because of the higher rate of $b\bar{b}$ events included in this sample, which leads to a shift of the maximum of the ξ distribution, ξ^*, to smaller values. Values of $\Lambda_{\rm eff} = 210 \pm 8$ MeV and -0.55 ± 0.03 for the $\mathcal{O}(1)$ correction to $< \xi >$ are obtained for the energy independent parameters. Here $N_F = 3$ was chosen since light quarks dominate quark pair production in the cascade. Including the Z data yields a slightly smaller $\Lambda_{\rm eff}$ and a value of χ^2/dof of 129/101.

MLLA also provides a definite prediction for the energy evolution of ξ^*. As hadronization and resonance decays are expected to act similarly at different centre-of-mass energies, the energy evolution of ξ^* is expected to be less sensitive to nonperturbative effects. A

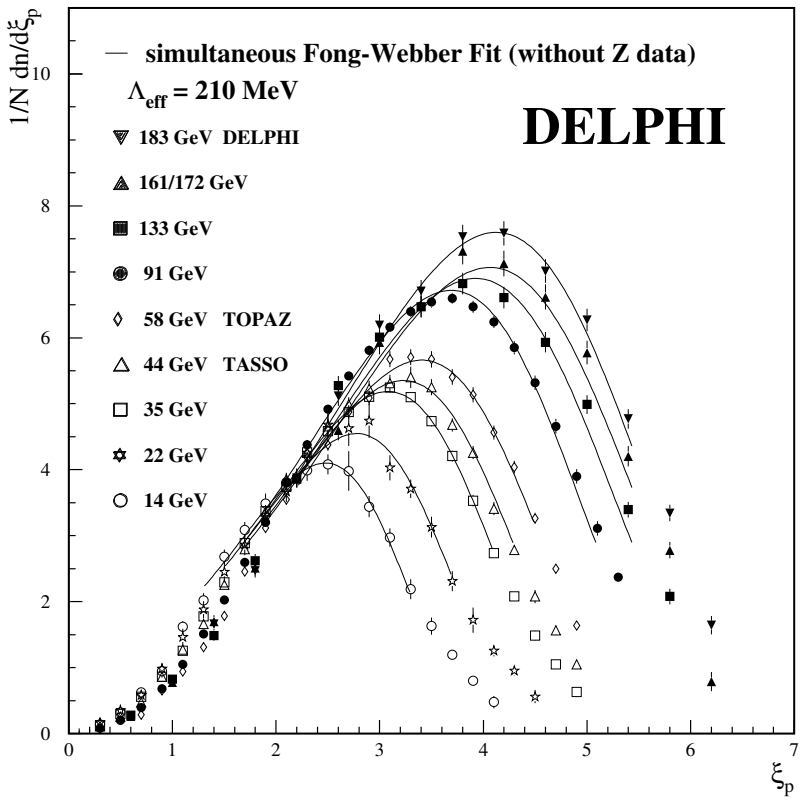

Figure 4: ξ_p distributions for charged particles. The full lines present the results of a simultaneous fit of the Fong-Webber parametrisation (2). The curves are drawn over the range of the fit ($\approx 50\%$ of the maximum height).

small correction is to be expected, however, due to varying contribution of heavy quark events. These chain decays are known to shift ξ^* in a way different from ordinary resonance decays. This shift also differs for the individual stable particle species due to their different masses. In this paper the influence of heavy decays is neglected.

The ξ^* values entering in this analysis were determined by fitting a distorted Gaussian with the parameters s, k, $< \xi >$ and σ given by the Fong-Webber calculation. The fit range in ξ is restricted to the part of the distribution close to the maximum with $1/\mathrm{N}\ \mathrm{dn}/\mathrm{d}\xi_p \geq 0.6\ (1/\mathrm{N}\ \mathrm{dn}/\mathrm{d}\xi_p)_{\mathrm{max}}$. To avoid systematic differences due to different strategies for the ξ^* determination, this fit has also been performed at the other energies [20,21]. The ξ^* values obtained are given in the table 3. The full line in Fig. 5 shows a fit of the MLLA prediction

$$\xi^* = 0.5 \cdot Y + \sqrt{C} \cdot \sqrt{Y} - C + \mathcal{O}(Y^{-\frac{3}{2}}) \tag{3}$$

to the data.

From this fit $\Lambda_{\mathrm{eff}} = 200 \pm 3$ MeV. This is in good agreement with the Λ_{eff} value obtained from the fit to the whole spectra. The quantity $C = \frac{\rho^2}{48\beta}$ depends on the number of active flavours ($C(N_F = 3) = 0.2915$, $C(N_F = 5) = 0.3513$). The results are presented for $N_F = 3$. The dashed line in Fig. 5 represents the slope of the phase space expectation

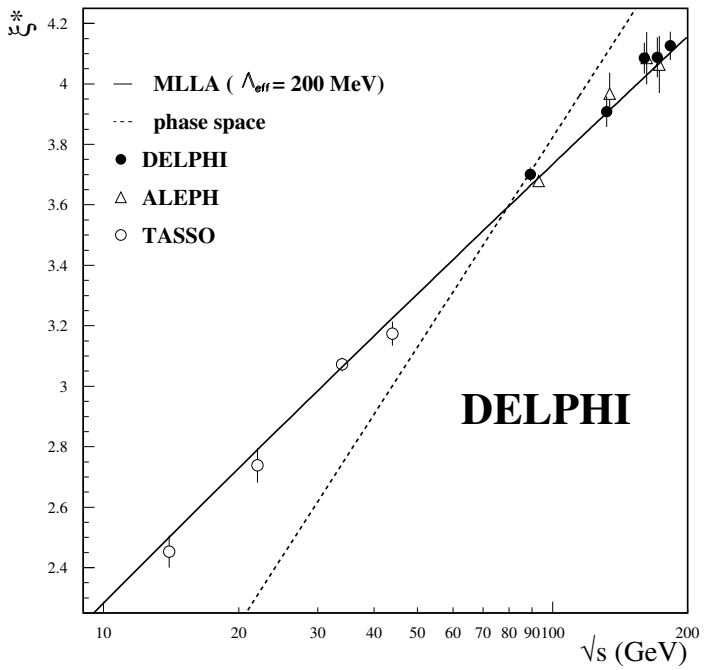

Figure 5: Energy evolution of the ξ_p peak position. $\Lambda_{\rm eff}$ is obtained from a fit to the MLLA/LPHD prediction. The phase space prediction is described in the text.

$\xi^* = a + Y$ [22]. Due to angular ordering of gluon bremsstrahlung the rise in ξ^* is slower in the MLLA prediction.

The MLLA provides also a prediction for the deviation of ξ^* and the mean $< \xi >$. Its value is 0.351(0.355) for $N_F = 3(5)$, independent of E_{CM} [23]. Since the ξ_p shape is symmetric in the Double Logarithmic Approximation (DLA), this deviation is in principle sensitive to the effect of single logarithmic terms [23]. It turns out that the determination of $< \xi >$ is not straightforward: integrating over the whole ξ_p spectrum would disregard the fact that the theoretical prediction is only valid around the region of the maximum. Therefore $< \xi >$ was obtained by fitting the distorted Gaussian with $< \xi >$ entering as a free parameter in the maximum region, defined by the condition $1/\mathrm{N}\ \mathrm{dn}/\mathrm{d}\xi_p \geq 0.5\ (1/\mathrm{N}\ \mathrm{dn}/\mathrm{d}\xi_p)_{\rm max}$. Table 3 shows the results. The weighted mean value of ξ^* - $< \xi >$ for the various energies results in 0.27 ± 0.03.

3.3 Energy Dependence of the Momentum Distribution

As the scaled momentum distribution may veil effects with an absolute scale, the evolution of the differential cross–section in absolute momentum p is also of interest. In Fig. 6 a) the momentum spectra obtained for the different centre-of-mass energies and the corresponding predictions of the JETSET model are compared.

For the low energy and Z data the spectra are obtained by rescaling the x_p distribution [6,12,19,24]. The energy evolution is well described by the fragmentation model. The most obvious feature is the increase of the distributions at large hadron momentum with energy. This is simply due to the enlarged phase space. A more interesting feature

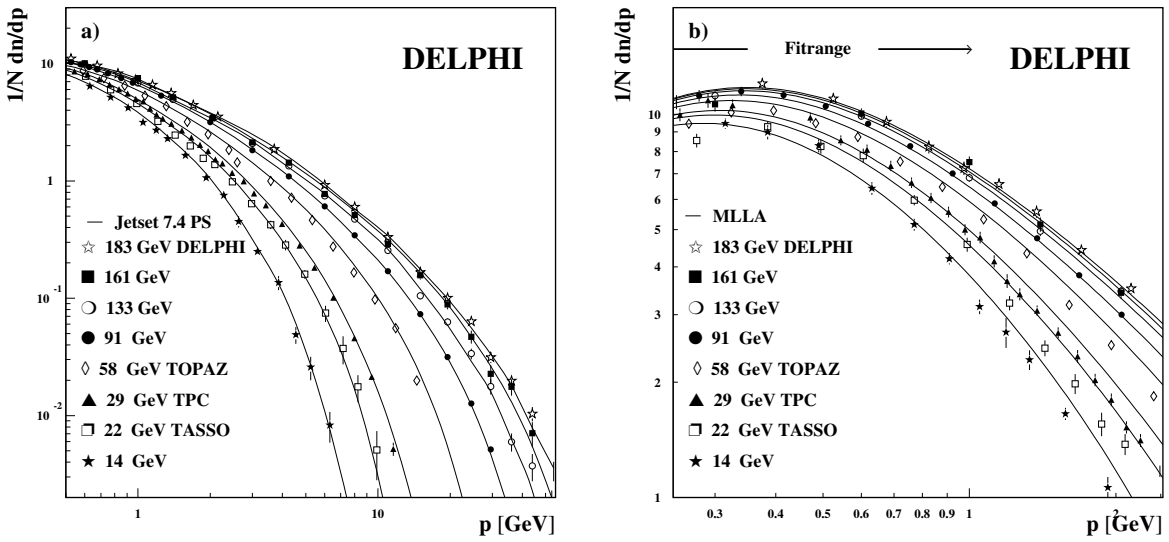

Figure 6: a) 1/N dn/dp distribution compared to JETSET for $p \leq 55$ GeV and b) to MLLA/LPHD prediction for $p \leq 2.5$ GeV. The parameter values of this fit are given in the last row of table 4

is the approximate $E_{\rm CM}$ independence of hadron production at very small momentum $p < 1$ GeV. This behaviour has been explained in [25] to be due to the coherent emission of low energy (i.e. long wavelength) gluons by the total colour current. This colour current is independent of the internal jet structure and conserved under parton splittings. Therefore low energy gluon emission is expected to be almost independent of the number of hard gluons radiated and hence of the centre-of-mass energy. As a consequence, the number of produced hadrons at small momentum is approximately constant.

In its range of validity ($p \leq 1$GeV) this prediction [25] is compared to the data in Fig. 6 b). It depends on the cutoff parameter Q_0, $\lambda = \log(Q_0/\Lambda_{\rm eff})$ and the normalisation K_H which relates parton and hadron distributions according to the LPHD hypothesis. It should be noted, that in contrast to the ξ_p calculations this prediction is *not* obtained in the "limited spectrum" ($\Lambda_{\rm eff} = Q_0$) approximation.

The curves in Fig. 6 b) correspond to a simultaneous fit of all DELPHI data from 91 to 183 GeV. Fitting all data or only the low energy data yields different values (especially in the logarithmic variable λ), but it should be noted that these parameters are highly correlated. Table 4 shows the different fit results. The large χ^2/dof for the fits of the low energy data compared to the satisfactory χ^2/dof for the DELPHI data may indicate systematic discrepancies between the measurements of the different experiments. Also the agreement with the MLLA/LPHD prediction is only expected to be qualitive, since many non-perturbative effects should be beyond its predictive power.

4 Summary

Inclusive charged hadron distributions as obtained from the DELPHI measurements at 130, 136, 161, 172 and 183 GeV are presented. Fragmentation models tuned at the Z describe the data well at higher energies. The energy evolution of the rapidity distribution

shows that the increase in multiplicity is to a large extent due to the growth in the plateau height. MLLA calculations in the limited spectrum approximation ($\Lambda_{\rm eff} = Q_0$) allow the ξ_p distribution and the energy dependence of its maximum to be parameterised. A new calculation [25] for the soft part of the partonic momentum spectrum is able to describe the hadronic p distribution in the range of small momenta. All these measurements yield values for $\Lambda_{\rm eff}$ from 200 to 236 MeV. This supports the assumption of local parton hadron duality.

Acknowledgements

We thank W. Ochs for helpful discussions and S. Lupia for providing us with the code for the $\frac{dn}{dp}$ calculation.
We are greatly indebted to our technical collaborators, to the members of the CERN-SL Division for the excellent performance of the LEP collider, and to the funding agencies for their support in building and operating the DELPHI detector.
We acknowledge in particular the support of
Austrian Federal Ministry of Science and Traffics, GZ 616.364/2-III/2a/98,
FNRS–FWO, Belgium,
FINEP, CNPq, CAPES, FUJB and FAPERJ, Brazil,
Czech Ministry of Industry and Trade, GA CR 202/96/0450 and GA AVCR A1010521,
Danish Natural Research Council,
Commission of the European Communities (DG XII),
Direction des Sciences de la Matière, CEA, France,
Bundesministerium für Bildung, Wissenschaft, Forschung und Technologie, Germany,
General Secretariat for Research and Technology, Greece,
National Science Foundation (NWO) and Foundation for Research on Matter (FOM), The Netherlands,
Norwegian Research Council,
State Committee for Scientific Research, Poland, 2P03B06015, 2P03B03311 and SPUB/P03/178/98,
JNICT–Junta Nacional de Investigação Científica e Tecnológica, Portugal,
Vedecka grantova agentura MS SR, Slovakia, Nr. 95/5195/134,
Ministry of Science and Technology of the Republic of Slovenia,
CICYT, Spain, AEN96–1661 and AEN96-1681,
The Swedish Natural Science Research Council,
Particle Physics and Astronomy Research Council, UK,
Department of Energy, USA, DE–FG02–94ER40817.

References

[1] Y. I. Azimov, Y. L. Dokshitzer, V. A. Khoze and S. I. Troyan, *Z. Phys.* **C27**(1985) 65.
[2] DELPHI Coll., P. Abreu et al., *Nucl. Instr. Meth.* **A303**(1991) 187.
[3] DELPHI Coll., P. Abreu et al., *Nucl. Instr. Meth.* **A378**(1996) 57.
[4] T. Sjöstrand, *Comp. Phys. Comm.* **39**(1986) 347.
[5] P. Abreu et al., "The Estimation of the Effective Centre of Mass Energy in $q\bar{q}\gamma$ Events from DELPHI", CERN-OPEN/98-026 (September 1998), submitted to Nucl. Instr. Methods A.
[6] DELPHI Coll., P. Abreu et al., *Z. Phys.* **C73**(1996) 11.
[7] TASSO Coll., W.Braunschweig et al., *Z.Phys.* **C41**(1988) 359.
[8] MARK II Coll., A.Petersen et al., *Phys.Rev.* **D37**(1988) 1.
[9] AMY Coll., Lie et al., *Phys.Rep.* **D41**(1990) 2675.
[10] TASSO Coll., M.Althoff et al., *Z.Phys.* **C22**(1984) 307.
[11] AMY Coll., H.Zheng et al., *Phys.Rev.* **D42**(1990) 737.
[12] TASSO Coll., W.Braunschweig et al., *Z. Phys.* **C47**(1990) 187.
[13] DELPHI Coll., P. Abreu et al., *Z. Phys.* **C 70**(1996) 179.
[14] DELPHI Coll., P. Abreu et al., *Phys. Lett.* **B 372**(1996) 172.
[15] DELPHI Coll., P. Abreu et al., *Phys. Lett.* **B 416**(1998) 233.
[16] DELPHI Coll., P. Abreu et al., Ref. #287 contributed to the ICHEP conference in Vancouver, 1998.
[17] Y. L. Dokshitzer, V. A. Khoze and S. I. Troyan, *Z. Phys.* **C55**(1992) 107.
[18] C. P. Fong and B. R. Webber, *Phys. Lett.* **B229**(1989) 289.
[19] TOPAZ Coll., R. Itoh et al., *Phys. Lett.* **B345**(1995) 335.
[20] ALEPH Coll., Ref. #629 contributed to the EPS HEP conference in Jerusalem, 1997.
[21] ALEPH Coll., R. Barate et al., *Phys.Rep.* **294**(1998) 1.
[22] B.R.Webber, Hadronization. Lectures at Summer School on Hadronic Aspects of Collider Physics, Zuoz, Switzerland, hep-ph/9411384, 1994.
[23] Y.L.Dokshitzer, V.A.Khoze, C.P.Fong and B.R.Webber, *Phys.Lett.* **B273**(1991) 319.
[24] TPC/2γ Coll., Aihara et al., *Phys. Rev. Lett.* **61**(1988) 1263.
[25] V. Khoze, S. Lupia and W. Ochs, *Phys. Lett.* **B394**(1997) 179.

E_{CM} [GeV]	ξ^*	$<\xi>$	ξ^* - $<\xi>$
14	2.453 ± 0.053	2.29 ± 0.04	0.16 ± 0.07
22	2.738 ± 0.057	2.16 ± 0.18	0.58 ± 0.10
35	3.072 ± 0.023	2.70 ± 0.05	0.37 ± 0.05
44	3.174 ± 0.039	2.91 ± 0.05	0.26 ± 0.06
91	3.701 ± 0.023	3.45 ± 0.02	0.26 ± 0.03
133	3.908 ± 0.051	3.74 ± 0.07	0.17 ± 0.08
161	4.085 ± 0.051	3.67 ± 0.20	0.42 ± 0.21
172	4.088 ± 0.066	3.52 ± 0.53	0.57 ± 0.54
183	4.126 ± 0.047	3.75 ± 0.15	0.38 ± 0.07
mean value:			0.27 ± 0.03

Table 3: The peak position, ξ^*, the mean value $<\xi>$ of the ξ_p distribution, and the difference of the two.

fitted energies [GeV]	Q_0 [MeV]	$\lambda = \log(Q_0/\Lambda_{\mathrm{eff}})$	K_H	χ^2/dof
all (14 - 183)	210 ± 4	0.095 ± 0.009	0.86 ± 0.04	179/57
low (14 - 58)	228 ± 4	0.055 ± 0.008	0.71 ± 0.04	118/34
DELPHI (91.2 - 183)	238 ± 3	0.010 ± 0.004	0.42 ± 0.04	13.4/20

Table 4: Parameters obtained from simultaneous fits of the LPHD/MLLA prediction to the momentum spectra at different energies.